Tetrahedron xxx (2016) 1–4

Contents lists available at ScienceDirect

Tetrahedron

journal homepage: www.elsevier.com/locate/tet

An unusual intramolecular *trans*-amidation

Heriberto Rivera, Jr.[a,†], Sachin Dhar[a,†], James J. La Clair[a], Shiou-Chuan Tsai[b,c,d,*], Michael D. Burkart[a,*]

[a] Department of Chemistry and Biochemistry, University of California, San Diego, 9500 Gilman Drive, La Jolla, CA 92093-0358, United States
[b] Department of Molecular Biology and Biochemistry, University of California, Irvine, CA 92697, United States
[c] Department of Chemistry, University of California, Irvine, CA 92697, United States
[d] Department of Pharmaceutical Sciences, University of California, Irvine, CA 92697, United States

ARTICLE INFO

Article history:
Received 25 August 2015
Received in revised form 27 January 2016
Accepted 30 January 2016
Available online xxx

Keywords:
trans-Amidation
Polyketide
Cyclization
Intramolecular reactions
Reaction mechanisms

ABSTRACT

Polyketide biosynthesis engages a series of well-timed biosynthetic operations to generate elaborate natural products from simple building blocks. Mimicry of these processes has offered practical means for total synthesis and provided a foundation for reaction discovery. We now report an unusual intramolecular *trans*-amidation reaction discovered while preparing stabilized probes for the study of actinorhodin biosynthesis. This rapid cyclization event offers insight into the natural cyclization process inherent to the biosynthesis of type II polyketide antibiotics.

1. Introduction

The mechanisms guiding polyketide biosynthesis have served as inspiration for both total synthesis[1] and reaction development efforts.[2] Within recent years, the fusion between synthetic organic chemistry and structural biology has provided a rich forum to further explore the mechanisms that guide each of the discrete operations during a biosynthetic process.[3] The significance of these advances has most recently allowed chemoenzymatic methods to address the total synthesis of complex natural products such as spinosyn A.[4]

One of the key complications encountered when studying intermediate formation within natural product biosynthesis arises from compound instability. This is particularly problematic in type II polyketide biosynthesis, as the formation of the acyl carrier protein (ACP) tethered polyketones such as **1a** (Fig. 1), are highly unstable.[5]

Similar problems with instability also arise after the cyclization begins, as intermediates such as **2a** are prone to uncontrolled aldol-type cyclizations, if not regulated. Our current hypothesis supports the concept that the ACP serves to both protect unstable cargo (**1a**, Fig. 1) as well as guide these species to the enzymes, which will catalyze specific cyclization events (Fig. 2). Interested in further understanding these processes at the structural level, we turned to the preparation of 'atom replacement probes'.[6]

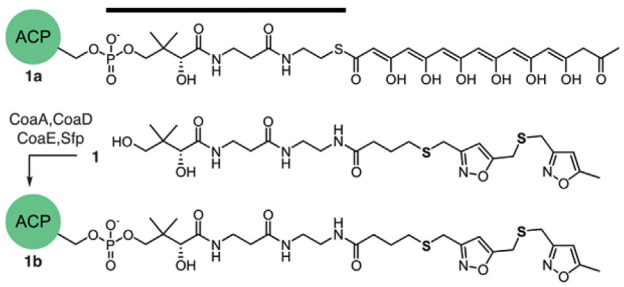

Fig. 1. Exemplary ketide acyl-carrier protein (ACP) tethered intermediate **1a** along with the corresponding stabilized atom replacement probe **1** and probe-loaded ACP **1b**. The black bar denotes the 4′-phosphopantetheinyl arm.

Through these studies, we learned that one could effectively prepare pantetheinylated mimetics of polyketones by the selective replacement of specific carbonyls with heteroatoms. As depicted in **1** (Fig. 1), we prepared probes bearing both thioethers and isoxazoles to represent key carbonyl units within the polyketone **1a**.[6] Similarly, we also developed partially-cyclized intermediates of **2a**, as shown in **2** (Fig. 2).

* Corresponding authors. E-mail addresses: sctsai@uci.edu (S.-C. Tsai), mburkart@ucsd.edu (M.D. Burkart).
† These authors contributed equally to the work.

http://dx.doi.org/10.1016/j.tet.2016.01.062
0040-4020/

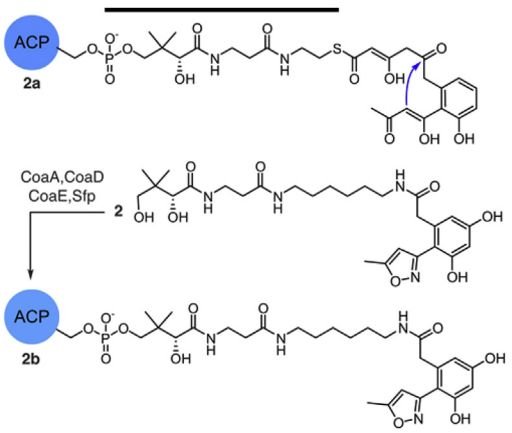

Fig. 2. Exemplary cyclized intermediate **2a** along with its associated atom replacement probe **2** and probe loaded ACP **2b**. The black bar denotes the 4′-phosphopantetheinyl arm.

Using the actinorhodin biosynthetic system as a model (Fig. 3), we were able to demonstrate that probes **1** and **2** can be loaded onto their ascribed ACP as given by the conversion of **1** to **1b** (Fig. 1) and **2** to **2b** (Fig. 2). As part of this study, we were able to apply solution-based protein NMR methods to demonstrate that intermediates **1b** and **2b** did indeed provide viable mimetics of their corresponding naturally-loaded **1a** and **2a**, respectively.[6] Overall, we were able to synthesize stable mimetics of intermediates at two stages of the actinorhodin biosynthetic process (Fig. 3).

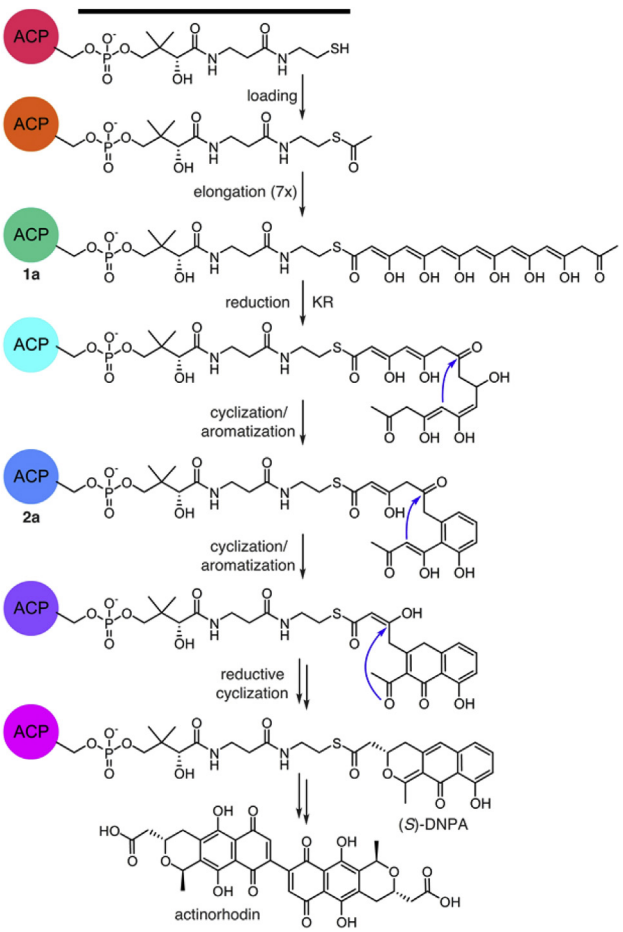

Fig. 3. Proposed biosynthesis of actinorhodin from *holo*-actACP.[6] One of the enol/ketol tautomerization states has been depicted. In solution, multiple tautomers exist. The processing of substrates on the actACP has been depicted by a color change of the sphere representing the ACP from red to violet with states **1a** and **2a** shown in Figs. 1 and 2, respectively.

2. Results and discussion

As part of this effort, we were interested in exploring the stability of ketides arising from opening of the isoxazole motif. Our plan was to use the isoxazole as a tool to mimic 1,3-dicarbonyl units, and hence restrict access to unwanted spontaneous aldol reactions. Our goal was to deliver a series of bench stable mimetics that could be used for structural biological studies. We began by preparing linear and cyclized mimetics and examining their incorporation on actACP by NMR.[7] We then examined what would happen upon opening of the isoxazole. To this end, we were able to open the isoxazole in simpler intermediates such as **3** providing imine **4** and diketide **5** (Fig. 4) in a sequential fashion. While not unexpected, this process was not possible with more complicated materials such as **1** (Fig. 1), which underwent rapid degradation. LC-MS monitoring of the cleavage process using probes such as isoxazole **1** clearly showed the rapid formation of multiple products immediately after treatment with $Mo(CO)_6$, indicating that even the imine-type intermediates were highly-reactive. We then turned to explore if this process was possible on our partially-cyclized materials, such as probe **2** (Fig. 2).

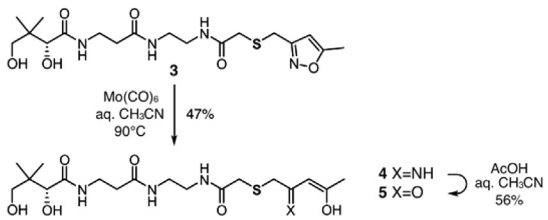

Fig. 4. Isoxazole cleavage. Ring opening of isoxazole **3** results in enaminone **4**, which in turn is hydrolytically-converted to ketide **5**.

2.1. Precursor synthesis

We began by examining materials from our recent studies.[7] Beginning with **6**[7] (Scheme 1), we were able to selectively deprotect the acetal by treatment in aq AcOH at rt to provide mimetic **7**. Treatment of **7** with fresh $Mo(CO)_6$ in refluxing aq CH_3CN[8] resulted in a clean conversion to enaminone **8** in an overall 86% yield from **6**.

2.2. Intramolecular *trans*-amidation of benzyl-protected enaminone 8

While stable thermally, exposure of **8** to mild acidic conditions (aq AcOH in CH_3CN) resulted in a crude product that lacked mass spectral signatures of the desired ketone. NMR monitoring of this reaction (Fig. 5) indicated the formation of two major materials, one of which was pantetheinamine **9**[9] (Scheme 1 and Supplementary Figs. S6–S8). The remaining material was attributed to **10**, as given by the presence of a compound containing two distinct benzylic groups in the crude NMR spectrum. Mass spectral analysis returned a formula of $C_{26}H_{23}NO_4$, indicating that **10** contained all of the remaining hydrogen, carbon, nitrogen and oxygen atoms of **8** ($C_{37}H_{46}N_4O_8$) after the elimination of **9** ($C_{11}H_{23}N_3O_4$).

Following purification of **10**, 1D NMR and 2D NMR analysis allowed complete assignment of the ^1H and ^{13}C spectra (see Supplementary data). As summarized on the left of Fig. 6, the ^{13}C data was suggestive of the structure of 1,4-dihydroisoquinolin-3(2H)-one motif bearing an exocyclic α,β-unsaturated ketone.

Please cite this article in press as: Rivera, H.; Jr.et al., Tetrahedron (2016), http://dx.doi.org/10.1016/j.tet.2016.01.062

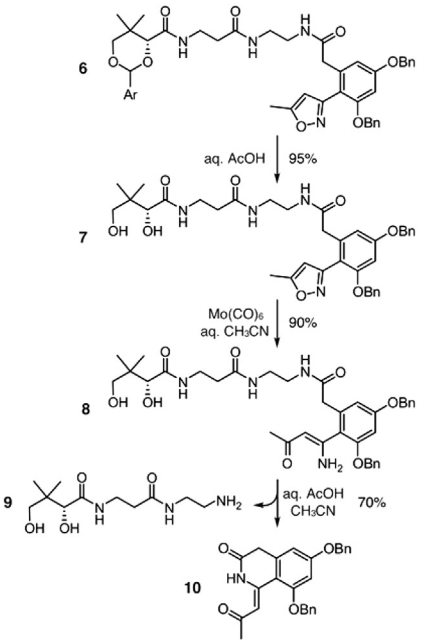

Scheme 1. Advance of cyclic mimetic **6**. Samples of **8** can be prepared two steps and in excellent yield from **6**. While stable to heat, compound **8** readily undergoes intramolecular *trans*-amidation resulting the formation of adduct **10** at rt under mildly acidic conditions.

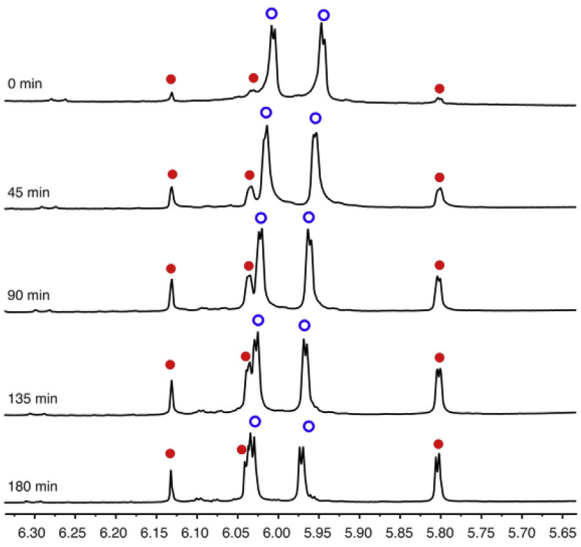

Fig. 5. ^{1}H NMR time course analysis depicting the conversion of **8** (blue circles) to **10** (red spheres) in 2:2:1 CD_3OOD:D_2O:CD_3OD. An expansion of the region between 5.60 and 6.35 ppm has been provided. Full spectral data has been provided in Supplementary Figs. S6–S8.

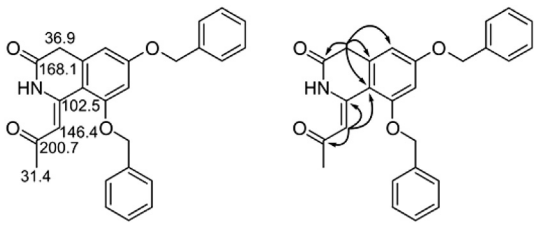

Fig. 6. NMR data confirming the assignment of **10**. (left) Select ^{13}C NMR assignments and (right) select ^{1}H, ^{13}C HMBC correlations.

Specifically, the data provided strong support for the exocyclic α,β-unsaturated ketone due to the presence of the chemical shift for the carbonyl at 200.7 ppm, the α-carbon at 146.4 ppm, and β-carbon at 102.5 ppm. Further evidence for the 1,4-dihydroisoquinolin-3(2H)-one core was also obtained by the ^{13}C peaks at 36.9 and 168.1 ppm. These assignments were further supported by HMBC correlations, as shown at the right of Fig. 6.

3. Conclusion

Ongoing efforts have recently led to the development of stabilized probes for studying intermediate processing within polyketide biosynthesis. While some atom replaced motifs provide sufficient stability (Fig. 4), others due to their access to rapid intramolecular cyclizations still lack sufficient stability (Scheme 1). Here, we report on a rather rare example of an intramolecular *trans*-amidation reaction. As illustrated in Scheme 1, the conversion of **8** to **10** occurred within 4 h at 23 °C under mildly acidic conditions. This suggests a strong driving force intrinsically built within the cyclic framework within atom-replacement probe **8**. While an uncommon event, the *trans*-amide formation observed herein (Scheme 1) not only demonstrates a unique reactivity but also provides a further means to synthetically-divert polyketide biosynthetic methods to enable access to new motifs, such as **10**. This finding suggests another alternative pathway that, while not accessed by the synthase, outlines the inherent non-enzyme catalyzed reactivity within the highly-reactive intermediates in polyketide biosynthesis. Mining these reactions not only expands the molecular diversity available through biosynthetic processes but also offers access to new structural motifs, a key step in expanding the utility of natural products. Overall, this study supports the importance of understanding polyketide biosynthesis not only by offering a means to comprehend and optimize natural product biosynthesis, but also by providing a platform for the advance of biosynthetically-derived natural product-like scaffolds.[10]

4. Experimental section

4.1. General

Unless otherwise noted, all reagents and chemical compounds were purchased from Alfa Aesar, Strem Chemicals, Sigma–Aldrich, Cambridge Isotopes or TCI and used without further purification. Flash chromatography was carried out on 40–63 mesh Geduran Silica Gel 60 (EMD Millipore). Thin layer chromatography (TLC) was conducted on 250 μm Silica Gel 60 F254 glass plates (EMD Millipore). NMR spectra were recorded on a Mercury Plus 400 MHz (Varian), a ECA 500 MHz (Jeol), a DMX 400 MHz (Bruker), a DMX 500 MHz (Bruker) or a VX 500 MHz equipped with XSens cold probe (Varian) spectrometer. FID files were processed using MestRenova version 10.0.1 (MestreLab Research). Mass spectrometric analyses were conducted on the following instruments: a LCQ Deca (ThermoFinnigan), MAT900XL (ThermoFinnigan), LTQ Orbitrap XL (ThermoScientific), or a LCT Premier (Waters) mass spectrometer. Reactions were conducted under Ar atmosphere in a round bottom flask or vial capped with a rubber septa and were stirred using a Teflon coated stir bar. All mixtures are provided as v:v ratios.

4.2. Experimental procedures and data of synthetic intermediates

4.2.1. Isoxazole **7**. PMB-protected isoxazole **6** (54.0 mg, 0.0683 mmol) was dissolved in 1 mL of 4:1 AcOH:H_2O. The solution was stirred for 4 h, after which starting material was no longer present by TLC analysis using 1:9 MeOH/CH_2Cl_2. Solvent was azeotropically removed by rotary evaporation with addition of

toluene (3×5 mL). Flash chromatography (CH_2Cl_2 to 1:9 MeOH:CH_2Cl_2) provided 43.6 mg (95%) of isoxazole **7**; TLC R_f=0.5 (silica gel, MeOH:CH_2Cl_2 1:9); ^{1}H NMR (500 MHz CDC1_3) 7.45–7.26 (m, 10H), 6.64 (d, *J*=2.3 Hz, 1H), 6.63 (d, *J*=2.3 Hz, 1H), 6.14 (d, *J*=1.0 Hz, 1H), 5.08 (s, 2H), 5.06 (s, 2H), 4.64 (br s, 1H), 3.88 (s, 1H), 3.64 (dddd, *J*=3.7, 6.9, 6.9, 13.8 Hz, 2H), 3.54–3.35 (m, 5H), 3.16 (ddd, *J*=2.6, 5.8, 14.1 Hz, 2H), 3.13 (ddd, *J*=3.3, 8.2, 14.0 Hz, 2H), 2.47 (d, *J*=1.0 Hz, 3H), 2.35 (m, 2H), 1.02 (s, 3H), 0.88 (s, 3H); ^{13}C NMR (125 MHz, $CDCl_3$) 174.0, 172.2, 172.1,* 172.0,* 169.1, 160.9, 159.6, 158.5, 136.7, 136.3, 136.3, 128.8, 128.7, 128.4, 128.2, 127.8, 127.0, 111.8, 108.7, 104.9, 100.4, 77.9, 71.1, 70.6, 70.4, 42.6, 39.8, 39.7,* 39.5, 39.3, 39.2,* 36.1, 35.3, 22.4, 20.4, 12.4; HRMS (*m*/*z*): $[M+H]^+$ calcd for $C_{37}H_{44}N_4O_8+H^+$ 673.3232; found 673.3230. Multiple confirmations of **7** were observed during NMR analysis with duplicate NMR signatures indicated above by an asterisk.

*4.2.2. Enaminone **8**.* Isoxazole **7** (40.0 mg, 0.0595 mmol) was dissolved in 2 mL of 3:1 MeCN:H_2O in 10 mL Teflon tube (Nalgene Oak Ridge Centrifuge Tubes). Solid $Mo(CO)_6$ (15.7 mg, 0.060 mmol) was added and the tube was flushed with Ar, capped, and warmed to 85 °C. TLC analysis using 1:9 MeOH:DCM indicated that consumption of starting material was complete within 6 h. The crude reaction mixture was transferred to a 50 mL round bottom flask and evaporated to dryness. Flash chromatography (CH_2Cl_2 to 1:9 MeOH:CH_2Cl_2) provided 36.1 mg (90% yield) of enaminone **8**; R_f=0.45 (silica gel, 1:9 MeOH:CH_2Cl_2); ^{1}H NMR (500 MHz CDC1_3) 7.39–7.24 (m, 10H), 6.99 (t, *J*=5.9 Hz, 1H), 6.75 (t, *J*=6.0 Hz, 1H), 6.55 (d, *J*=2.3 Hz, 1H), 6.54 (d, *J*=2.3 Hz, 1H), 5.08 (s, 1H), 5.05 (d, *J*=2.3 Hz, 1H), 5.02 (s, 2H), 3.79 (br s, 2H), 3.54–3.38 (m, 7H), 3.28 (m, 2H), 3.12 (dddd, *J*=5.3, 5.3, 5.3, 10.5 Hz, 2H), 2.30 (ddd, *J*=4.3, 7.4, 15.3 Hz, 1H), 2.20 (m, 1H), 2.06 (s, 3H), 0.95 (s, 3H), 0.86 (s, 3H); ^{13}C NMR (125 MHz, $CDCl_3$) 197.5, 174.9, 172.4, 172.1, 160.1, 159.8, 157.0, 136.6, 136.5, 135.0, 128.8, 128.7, 128.4, 128.0, 127.8, 127.0, 120.8, 108.4, 100.2, 98.1, 77.9, 71.0, 70.6, 70.3, 41.0, 40.0, 39.6, 39.3, 36.2, 35.3, 29.7, 21.7, 20.6; HRMS (*m*/*z*): $[M+H]^+$ calcd for $C_{37}H_{46}N_4O_8+H^+$ 675.3388; found 675.3389.

*4.2.3. Cyclized adduct **10**.* Enaminone **8** (20.0 mg, 0.0296 mmol) was dissolved in 2:2:1 AcOH:H_2O:MeCN and stirred at rt. TLC analysis using 1:9 MeOH:CH_2Cl_2 indicated consumption of starting material after 4 h. The crude reaction mixture was evaporated to dryness azeotropically with toluene (3×5 mL). Flash chromatography (CH_2Cl_2 to 1:5 CH_2Cl_2:MeOH) provided 8.6 mg (70% yield) of **10**; ^{1}H NMR (500 MHz CDC1_3) 12.69 (br s, 1H), 7.51–7.34 (m, 10H), 6.89 (s, 1H), 6.60 (d, *J*=2.4 Hz, 1H), 6.42 (d, *J*=2.4 Hz, 1H), 2.01 (s, 3H); ^{13}C NMR (125 MHz, $CDCl_3$) 200.7, 168.1, 161.7, 159.9, 146.4, 138.5, 135.9, 135.5, 128.9, 128.8, 128.6, 128.1, 127.7, 107.9, 106.2, 102.5, 100.2, 71.6, 70.5, 36.9, 31.4; HRMS (*m*/*z*): $[M+H]^+$ calcd for $C_{26}H_{23}NO_4+H^+$ 414.1700; found 414.1701.

4.3. NMR analysis of the conversion of enaminone 8 to cyclized adduct 10

Enaminone **8** (5.2 mg) was dissolved in 0.8 mL of 2:2:1 (AcOD:D_2O:CD_3CN) at rt. The reaction was monitored over the course of 24 h by ^{1}H NMR analysis on a VX 500 MHz equipped with XSens cold probe (Varian) spectrometer.

Acknowledgements

Funding for this project was provided by National Institutes of Health GM095970 and GM100305. We also thank Dr. Dr. X. Huang (UC San Diego), Dr. A. Mrse (UC San Diego), Dr. Y. Su (UC San Diego) and Dr. P. Dennison (UC Irvine) for assistance with collection of NMR and MS data.

Supplementary data

Supplementary data associated with this article can be found in the online version, at http://dx.doi.org/10.1016/j.tet.2016.01.062.

References and notes

1. A selection of recent synthetic efforts that explore biomimetic approaches to polyketide total synthesis: (a) Barrett, T. N.; Barrett, A. G. *J. Am. Chem. Soc.* **2014**, *136*, 17013–17015; (b) Hager, A.; Mazunin, D.; Mayer, P.; Trauner, D. *Org. Lett.* **2011**, *13*, 1386–1389; (c) Norris, M. D.; Perkins, M. V.; Sorensen, E. J. *Org. Lett.* **2015**, *17*, 668–671.
2. See the following articles for examples of biosynthetically-inspired method development (a) Aquino, C.; Sarkar, M.; Chalmers, M. J.; Mendes, K.; Kodadek, T.; Micalizio, G. C. *Nat. Chem.* **2011**, *4*, 99–104; (b) Pan, Y.; Kee, C. W.; Jiang, Z.; Ma, T.; Zhao, Y.; Yang, Y.; Xue, H.; Tan, C. H. *Chemistry* **2011**, *17*, 8363–8370; (c) Zheng, K.; Xie, C.; Hong, R. *Front. Chem.* **2015**, *3*, 1–17.
3. Kim, H. J.; Choi, S. H.; Jeon, B. S.; Kim, N.; Pongdee, R.; Wu, Q.; Liu, H. W. *Angew. Chem., Int. Ed.* **2014**, *53*, 13553–13557.
4. (a) Nguyen, C.; Haushalter, R. W.; Lee, D. J.; Markwick, P. R.; Bruegger, J.; Caldara-Festin, G.; Finzel, K.; Jackson, D. R.; Ishikawa, F.; O'Dowd, B.; McCammon, J. A.; Opella, S. J.; Tsai, S. C.; Burkart, M. D. *Nature* **2014**, *505*, 427–431; (b) Teufel, R.; Miyanaga, A.; Michaudel, Q.; Stull, F.; Louie, G.; Noel, J. P.; Baran, P. S.; Palfey, B.; Moore, B. S. *Nature* **2013**, *503*, 552–556; (c) Piasecki, S. K.; Zheng, J.; Axelrod, A. J.; Detelich, M. E.; Keatinge-Clay, A. T. *Proteins* **2014**, *82*, 2067–2077; (d) Bretschneider, T.; Heim, J. B.; Heine, D.; Winkler, R.; Busch, B.; Kusebauch, B.; Stehle, T.; Zocher, G.; Hertweck, C. *Nature* **2013**, *502*, 124–128; (e) Mori, T.; Yang, D.; Matsui, T.; Hashimoto, M.; Morita, H.; Fujii, I.; Abe, I. *J. Biol. Chem.* **2015**, *290*, 5214–5225; (f) Lee, M. Y.; Ames, B. D.; Tsai, S. C. *Biochemistry* **2012**, *51*, 3079–3091.
5. For studies that address the limits of polyketone stability see: (a) Fouché, M.; Rooney, L.; Barrett, A. G. *J. Org. Chem.* **2012**, *77*, 3060–3070; (b) Calo, F.; Richardson, J.; Barrett, A. G. *Org. Lett.* **2009**, *11*, 4910–4913; (c) Navarro, I.; Basset, J. F.; Hebbe, S.; Major, S. M.; Werner, T.; Howsham, C.; Bräckow, J.; Barrett, A. G. *J. Am. Chem. Soc.* **2008**, *130*, 10293–10298; (d) Harris, T. M.; Murray, T. P.; Harris, C. M.; Gumulka, M. *J. Chem. Soc., Chem. Commun.* **1974**, 362–363; (e) Harris, T. M.; Harris, C. M. *Tetrahedron* **1977**, *33*, 2159–2185.
6. While multiple intermediates can be drawn at each step of this process including different enol/ketol states, we presented this route based on evidence developed by the Malpartida and Hopwood laboratories. For further information, see: (a) Fernándes-Moreno, M. A.; Martínez, E.; Caballero, J. L.; Ichinose, K.; Hopwood, D. A.; Malpartida, F. *J. Biol. Chem.* **1994**, *269*, 24854–24863; (b) Kendrew, S. G.; Hopwood, D. A.; Marsh, E. N. G. *J. Bacteriol.* **1997**, *179*, 4305–4310.
7. Shakya, G.; Rivera, H., Jr.; Lee, D. J.; Jaremko, M. J.; La Clair, J. J.; Fox, D. T.; Haushalter, R. W.; Schaub, A. J.; Bruegger, J.; Barajas, J. F.; White, A. R.; Kaur, P.; Gwozdziowski, E. R.; Wong, F.; Tsai, S. C.; Burkart, M. D. *J. Am. Chem. Soc.* **2014**, *136*, 16792–16799.
8. (a) Nitta, M.; Kobayashi, T. *J. Chem. Soc., Chem. Commun.* **1982**, 877–878; (b) Anderson-McKay, J.; Savage, G. P.; Simpson, G. W. *Aust. J. Chem.* **1996**, *46*, 163–166.
9. Compound **9** was not isolated or characterized from this reaction. It was however detected in the NMR monitor of the conversion of **8** to **10**, as shown in Supplementary Figs. S6–S8.
10. (a) Jürjens, G.; Kirschning, A.; Candito, D. A. *Nat. Prod. Rep.* **2015**, *32*, 723–737; (b) Xu, Y.; Zhou, T.; Zhang, S.; Espinosa-Artiles, P.; Wang, L.; Zhang, W.; Lin, M.; Gunatilaka, A. A.; Zhan, J.; Molnár, I. *Proc. Natl. Acad. Sci. U.S.A.* **2014**, *111*, 12354–12359; (c) Walsh, C. T. *Acc. Chem. Res.* **2008**, *41*, 4–10.